Glycobiology vol. 0 no. 0 pp. 1–11, 2011
doi:10.1093/glycob/cwr158
Advance Access publication on Month 00, 0000

Antitumor effects of hyaluronic acid inhibitor 4-methylumbelliferone in an orthotopic hepatocellular carcinoma model in mice

Flavia Piccioni[2,3], Mariana Malvicini[2,3], Mariana G Garcia[2,3], Andrés Rodriguez[2], Catalina Atorrasagasti[2,3], Nestor Kippes[2], Ignacio T Piedra Buena[2], Manglio M Rizzo[2], Juan Bayo[2,4], Jorge Aquino[2,3], Manuela Viola[5], Alberto Passi[5], Laura Alaniz[1,2,3], and Guillermo Mazzolini[1,2,3]

[2]Gene Therapy Laboratory, School of Medicine, Austral University, Avenida Presidente Perón 1500 (B1629ODT) Derqui-Pilar, Buenos Aires, Argentina; [3]CONICET (Consejo Nacional de Investigaciones Científicas y Técnicas), Buenos Aires, Argentina; [4]Agencia Nacional de Promoción Científica y Tecnológica (ANPCyT), Buenos Aires, Argentina; and [5]Dipartimento di Scienze Biomediche Sperimentali e Cliniche, Universitá degli Studi dell'Insubria, via J.H. Dunant 5, 21100 Varese, Italy

Received on March 5, 2011; revised on October 17, 2011; accepted on October 20, 2011

Liver cirrhosis is characterized by an excessive accumulation of extracellular matrix components, including hyaluronan (HA). In addition, cirrhosis is considered a pre-neoplastic disease for hepatocellular carcinoma (HCC). Altered HA biosynthesis is associated with cancer progression but its role in HCC is unknown. 4-Methylumbelliferone (4-MU), an orally available agent, is an HA synthesis inhibitor with anticancer properties. In this work, we used an orthotopic Hepa129 HCC model established in fibrotic livers induced by thioacetamide. We evaluated 4-MU effects on HCC cells and hepatic stellate cells (HSCs) in vitro by proliferation, apoptosis and cytotoxicity assays; tumor growth and fibrogenesis were also analyzed in vivo. Our results showed that treatment of HCC cells with 4-MU significantly reduced tumor cell proliferation and induced apoptosis, while primary cultured hepatocytes remained unaffected. 4-MU therapy reduced hepatic and systemic levels of HA. Tumors systemically treated with 4-MU showed the extensive areas of necrosis, inflammatory infiltrate and 2–3-fold reduced number of tumor satellites. No signs of toxicity were observed after 4-MU therapy. Animals treated with 4-MU developed a reduced fibrosis degree compared with controls (F1-2 vs F2-3, respectively). Importantly, 4-MU induced the apoptosis of HSCs in vitro and decreased the amount of activated HSCs in vivo. In conclusion, our results suggest a role for 4-MU as an anticancer agent for HCC associated with advanced fibrosis.

Keywords: liver fibrosis / liver cancer / 4-methylumbelliferone

Introduction

Hyaluronan (HA) is a linear, large and ubiquitous non-sulfated glycosaminoglycan (GAG) of extracellular matrix (ECM) that can also be associated with cell surface (Toole 2004). The cellular effects of HA are mediated by different receptors, such as CD44 and RHAMM (Turley et al. 2002). HA is found in almost all tissues but especially increased in those undergoing cell proliferation, regeneration and repair, such as embryonic, inflamed and tumor stroma tissues (Toole 2002; Alaniz et al. 2009). HA can be present in different molecular weight (MW) species and associated with different biological functions. High MW (HMW) HA (10^6–10^7 Da) can play a physiological role participating in tissue homeostasis and in protein distribution in cell membrane. However, in certain pathological conditions such as injured tissues, low MW products ($0.1–1 \times 10^6$ Da) of HA are generated by differential expression of hyaluronidases (Stern 2005) as well as by oxidation process (Noble 2002; Tammi et al. 2002). Moreover, these products are supposed to contribute to scar formation and fibrogenesis (McKee et al. 1996; West et al. 1997; Guo et al. 2010).

The liver is responsible for the uptake and degradation of HA (Fraser et al. 1981). Under physiological conditions, systemic HA levels are low or undetectable; however, serum HA levels are increased in patients with liver fibrosis or cirrhosis (Vrochides et al. 1996). Liver fibrosis is a wound healing process that occurs in response to a number of hepatic diseases such as severe alcohol intake and chronic hepatitis (Bataller and Brenner 2005; Friedman 2008). As a result, there are changes in ECM composition and organization where activated hepatic stellate cells (HSCs) play a key role as the major collagen-ECM-producing cells in the damaged livers (Safadi and Friedman 2002; Friedman 2008). The accumulation of ECM components and advanced liver fibrosis may result in cirrhosis, hepatic failure and increased portal pressure and often require liver transplantation (Bataller and Brenner 2005). In addition, cirrhosis is a major risk factor for

[1]To whom correspondence should be addressed: Tel: +54-2322-482618; Fax: +54-2322-482204; e-mail: gmazzoli@cas.austral.edu.ar (G.M.)/laualaniz@yahoo.com.ar (L.A.)

the development of hepatocellular carcinoma (HCC; El-Serag and Rudolph 2007). Curative treatments can only be applied to a minority of patients at the time of diagnosis (Rampone et al. 2010). Therefore, new therapeutic options are urgently needed for advanced disease.

4-Methylumbelliferone (4-MU) is a 7-hydroxy-4-methyl coumarin, a molecule of vegetal origin that has been used safely in humans as a cholagogue orally as well as in clinical trials in patients with chronic hepatitis B and C (ClinicalTrials.gov identifier: NCT00225537; Takeda 1981). 4-MU has been used as a specific HA synthesis inhibitor in many in vitro studies (Yoshihara et al. 2005; Morohashi et al. 2006; Kultti et al. 2009). Its effect was first demonstrated in vitro in human fibroblasts, where the inhibition of HA synthesis but not other GAGs was observed (Kakizaki et al. 2004). Similar results were observed in B16F10 melanoma and KP1-NL human pancreatic cancer cells (Morohashi et al. 2006). Even though 4-MU action mechanism is not well-defined, this molecule can act through the reduction in HA synthase mRNA levels and by the depletion of HA synthesis precursors UDP-glucuronic acid as it has been observed in melanoma, breast and ovarian cancer cells (Kultti et al. 2009). It has been demonstrated in mice with melanoma that 4-MU selectively inhibits hepatic HA synthesis, resulting in the inhibition of liver metastases. The authors argued that HA formation on the cell surface is critical for tumor dissemination (Yoshihara et al. 2005). In addition, antitumoral effects of 4-MU have been reported for breast, esophageal and prostate carcinoma (Lokeshwar et al. 2010; Twarock et al. 2011; Urakawa et al. 2011). Therefore, we thought that the inhibition of HA synthesis by 4-MU in the injured liver and in HCC cells should help to control tumor growth and fibrosis progression.

Results

HA production and binding activity of HCC cells

We first analyzed HA-binding capacity, CD44 expression and HA production on HCC cells including the Hepa129 cell line. Hepa129 cells expressed CD44 (60.3%) and bound to HA (59.2%; Figure 1A). Binding is partially to CD44, because pretreatment with a monoclonal antibody (mAb) anti-CD44 (KM81, HA-blocking antibody) affected HA binding (from 59.2% to 45.4%; Figure 1A). In addition, we observed that Hepa129 cells highly secreted HA as detected by an enzyme-linked immunosorbent assay (ELISA)-like assay in culture supernatants (1940 ± 90 ng/mL/24 h; Figure 1B). We also analyzed these parameters in Hep3B and Huh7 human HCC cell lines and observed that they did not express CD44 and produced low amounts of HA in comparison with Hepa129 cells (1450 ± 60 and 500 ± 200 ng/mL/24 h, respectively) as assessed by an HA ELISA-like assay (Figure 1B).

In vitro 4-MU treatment inhibits cell proliferation and induces apoptosis in HCC cell lines and inhibits HA production

Effect of 4-MU on HCC growth is shown in Figure 2A (left panel). Hepa129 and Hep3B cells showed the inhibition of the proliferation in a dose-dependent manner. HCC cell proliferation was significantly reduced at a dose of 0.5 mM 4-MU for Hepa129 and Hep3B. In contrast, only higher doses of 4-MU (5 mM) were able to inhibit HuH7 cell proliferation (90% vs control). We next examined whether the growth inhibition by 4-MU was due to the induction of apoptosis (Figure 2A, right panel). 4-MU strongly induces apoptosis in Hepa129 and Hep3B cells at a dose of 5 mM (52 and 49%, respectively), whereas Huh7 were resistant to apoptosis in all

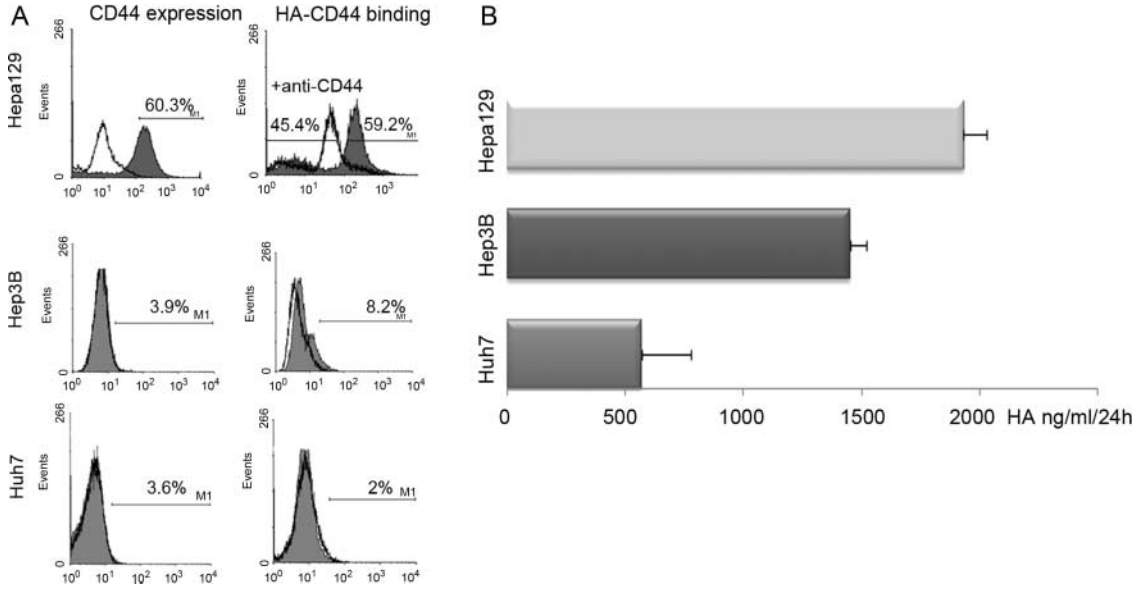

Fig. 1. HA binding and production by HCC cells. (**A**) Expression of CD44 by Hepa129, Hep3B and Huh7 (gray shade) and isotype control (black line). HA binds trough CD44 (gray shade). Black line represents displacement with anti-CD44 (KM81). This experiment is representative of three independent experiments. (**B**) Measurement of HA levels by HA ELISA-like assay. Cells (10^6/m) were cultured for 24 h and supernatants were analyzed for HA content. Data are expressed as the mean ± SEM (from three experiments).

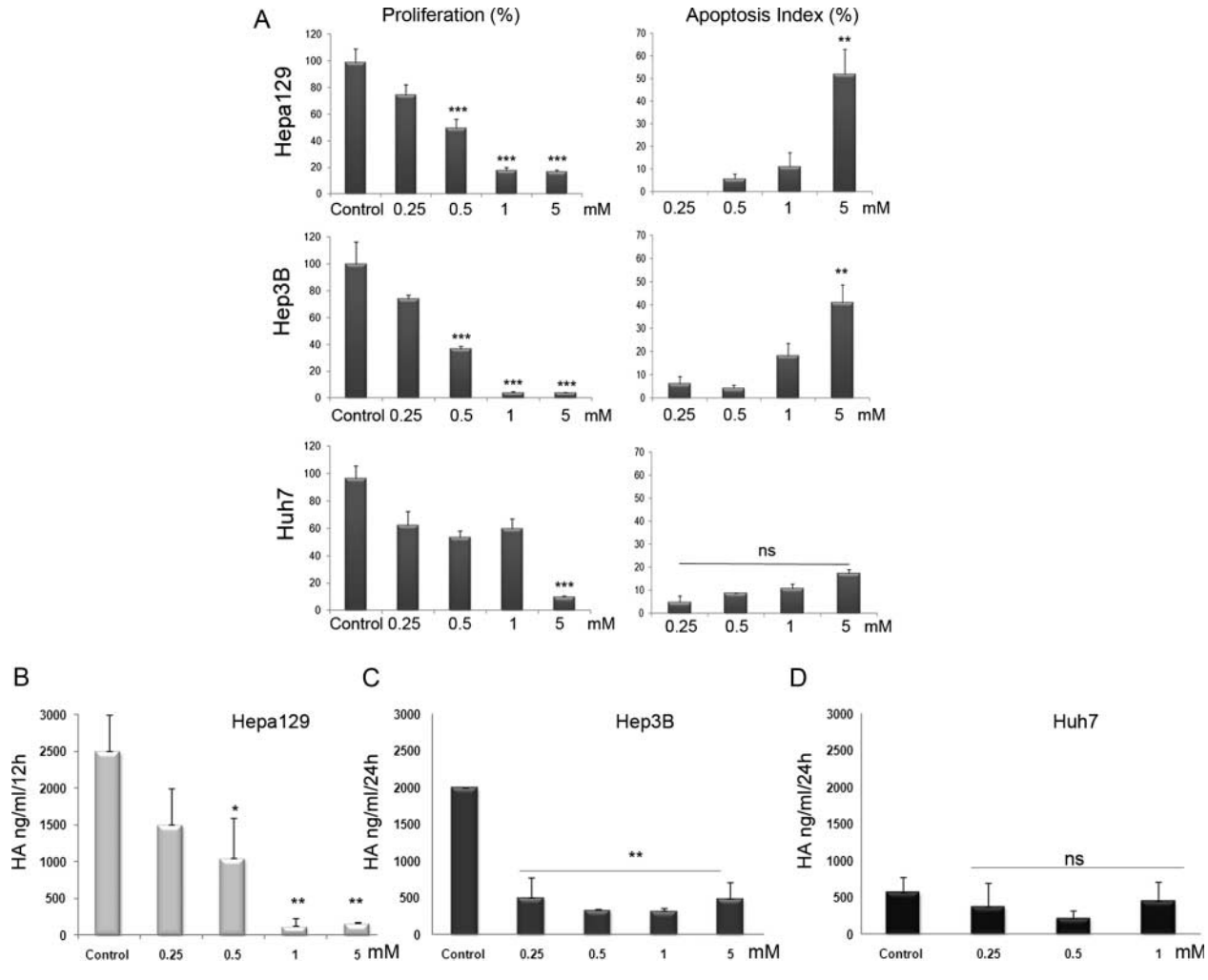

Fig. 2. Effect of 4-MU on HA synthesis, apoptosis and cell proliferation. (**A**) In vitro proliferation of HCC cells tested by ^{3}H-thymidine incorporation in three cell lines with different 4-MU concentrations (left panel). Control: HBSS medium. $*P < 0.05$, $**P < 0.01$ vs control without 4-MU. This experiment is representative of three independent experiments. Data are expressed as the mean ± SEM of proliferation average (measured in triplicate). Apoptosis was tested in vitro by morphological features using acridin orange/ethidium bromide (right panel). Apoptosis index: % Apoptosis 4-MU − % Apoptosis control. $*P < 0.05$, $**P < 0.01$ and $***P < 0.001$ vs control (not shown). Bars represent the average of measures of each group ± SEM. Experiments are shown as the average of three independent assays. Measurement of HA levels in Hepa129 (**B**), Hep3B (**C**) and Huh7 (**D**) cells by HA ELISA-like assay. Cells (10^{6}/mL) were cultured and treated for 12 h (Hepa129) or 24 h (Hep3B and Huh7) with different 4-MU concentrations, and supernatants were analyzed for HA content. Data are expressed as the mean ± SEM (from three experiments).

tested doses. Apoptosis results were confirmed by an Annexin V assay (data not shown). Hepa129 cells secrete higher HA levels when compared with Hep3B and Huh7 cells (Figure 1B). We therefore measured the effect of 4-MU on HA synthesis in Hepa129, Hep3B and Huh7 cells. As shown in Figure 2, 4-MU inhibited HA synthesis in both Hepa129 and Hep3B cell lines. For murine Hepa129 cells, inhibition of HA synthesis was significant at 12 h in comparison with control (Figure 2B), but not significant differences were observed at 24 h (data not shown). Human Hep3B cells shown a significant reduction in the HA level at 24 h in comparison with control (Figure 2C), whereas no reduction in the HA level was observed in Huh7 cells for the analyzed times (Figure 2D).

These results show that there is a correlation between HA synthesis and induction of apoptosis after treatment with 4-MU for Hepa129 and Hep3B cells, whereas the low-producer Huh7 cells were resistant to 4-MU-induced apoptosis.

Antitumoral effects of 4-MU in an orthotopic HCC model associated with advanced liver fibrosis

HCC tumors are frequently associated with advanced fibrosis or cirrhosis. To assess the effects of HA synthesis inhibition using 4-MU on HCC tumor development, we established an orthotopic tumor model (as described in *Materials and methods*, Figure 3A) associated with advanced fibrosis [induced by thioacetamide (TAA)] that is characterized by the presence of a main tumor mass and macroscopic tumor satellites. 4-MU therapy inhibited HCC tumor mass growth in mice with fibrosis in comparison with untreated animals,

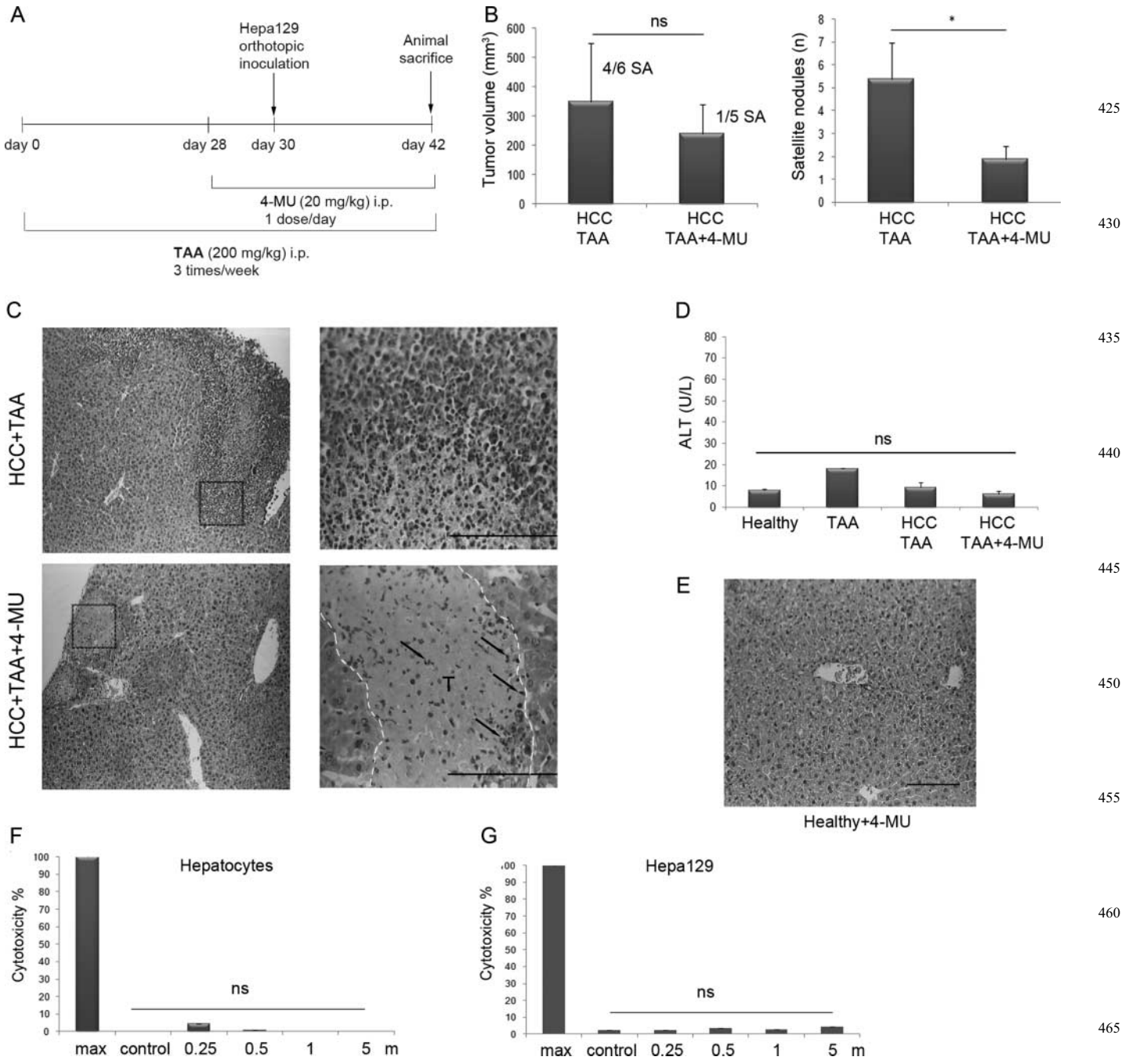

Fig. 3. Effect of 4-MU on Hepa129 tumors. (**A**) Experimental in vivo model. Fibrosis was induced in C3H/He mice by TAA i.p. injections three times per week for 42 days. Then, at day 30, Hepa129 HCC cells were implanted into the liver of fibrotic mice ($n = 6$/group). Treatment with 4-MU was started 2 days before the surgery, and injected i.p. once a day, up to animal sacrifice. (**B**) Tumor volume (mm^3) was measured in the liver from animals with fibrosis treated or not treated with 4-MU. Four of six animals with fibrosis and HCC but non-treated with 4-MU showed severe ascites (SA) in comparison with one of five animals treated with 4-MU. HCC satellites quantification: 4-MU reduced 2–3-fold the number of satellite nodules in comparison with 4-MU untreated mice with fibrosis and HCC. *$P < 0.05$ vs untreated. (**C**) Microphotography of H&E stained Hepa129 tumors from mice with fibrosis treated or not treated with 4-MU (10×). Magnification of tumor regions (40×) showing necrotic areas (showed as eosinophilic areas) in 4-MU-treated mice (arrows indicate some mononuclear inflammatory cells in the tumor edge; T, tumor). (**D**) Serum ALT (U/L) measurement showed that 4-MU treatment does not induce hepatocyte necrosis. (**E**) Representative liver section stained with H&E from a healthy mouse treated with 4-MU. Scale bar = 50 μm. Experiments were done in triplicate. ns, no significant. (**F**) Cytotoxicity analysis of 4-MU on a primary culture of murine hepatocytes was performed by LDH detection. Max, control of maximum lysis. (**G**) Cytotoxicity analysis of 4-MU on the murine HCC cell line Hepa129 was performed by LDH detection. Max, control of maximum lysis. Bars represent the average of measures of each group ± SEM. Experiments are shown as the average of three independent assays.

although these results were not statistically significant (350 vs 250 mm^3, respectively; Figure 3B). However, the number of satellite tumor nodules, as an indicator of tumor aggressiveness, was found ~2–3-fold reduced in 4-MU-treated mice (HCC + TAA + 4-MU group; Figure 3B). Interestingly, the majority of untreated mice (HCC + TAA group) developed severe ascites (including hemorrhagic ascites), whereas in the HCC + TAA + 4-MU group, ascites was almost absent or mild, as assessed by laparotomy. Importantly, microscopic examination of hepatic tumors revealed that mice treated with 4-MU showed increased mononuclear inflammatory cell infiltrate, which was more abundant in tumor edges and extensive areas of necrosis (Figure 3C) when compared with non-treated mice.

Toxicity studies

We then evaluated 4-MU toxicity in vitro and in vivo. Healthy mice treated with 4-MU showed no changes in body weight during the treatment course in comparison with healthy untreated mice (not shown). Serum chemistry analysis showed no significant differences in alanine transaminase (ALT) levels after treatment with 4-MU, indicating the absence of significant necrosis of hepatocytes after 4-MU administration (Figure 3D). 4-MU treatment did not cause any sign of hepatocellular damage and liver histology was normal (Figure 3E). To confirm these results, primary cultured hepatocytes treated with 4-MU were assessed for apoptosis and cytotoxicity. We observed that 4-MU did not affect hepatocytes in culture, since there were no significant differences in apoptosis between 4-MU doses (not shown) and cytotoxicity was lower than 5% (Figure 3F). In addition, 4-MU also showed no cytotoxic effect on Hepa129 cells (Figure 3G).

4-MU treatment reduced the amount of hepatic HA

HA expression was evaluated in liver tissue sections of mice from different groups by staining with an HA-binding protein (HA-BP). In healthy mice, the HA label was almost absent (Figure 4A). Contrarily, high HA expression was observed in liver sections from mice with established fibrosis or with both HCC and fibrosis (Figure 4A). As a result of 4-MU therapy, mice showed a remarkable reduction in HA expression, mainly inside HCC tumor nodules (Figure 4A). We then quantified HA by an ELISA-like assay in the liver tissue and, as expected, we observed a very significant reduction in the hepatic HA content after treatment with 4-MU in comparison with the livers from non-treated mice. This reduction was also seen when compared with mice with fibrosis alone (TAA group; Figure 4B). Accordingly, serum HA levels were also reduced after 4-MU therapy (Figure 4C).

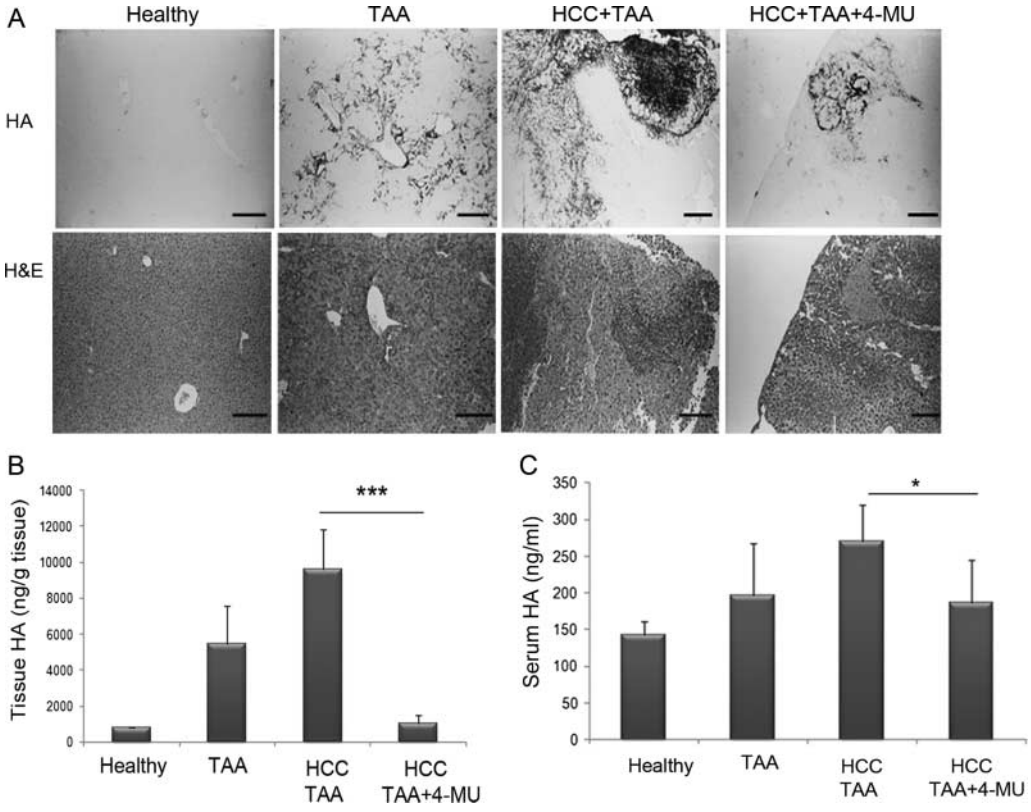

Fig. 4. Effects of 4-MU treatment on hepatic and systemic HA. (**A**) Hepatic HA staining by HA-BP. HA deposit is seen in black. General architecture of the liver tissue is seen by H&E staining. Scale bar = 50 µm. (**B**) Tissue HA quantification was performed from GAG extracts from the liver tissue and detected by HA ELISA-like assay and normalized to grams of tissue. ***$P < 0.001$. (**C**) Serum HA quantification was performed by HA ELISA-like assay. *$P < 0.05$. Bars represent the average of measures of each group ± SEM. Experiments are shown as the average of three independent assays.

4-MU treatment reduces liver fibrosis induced by TAA

We next decided to investigate whether 4-MU treatment may influence liver fibrogenesis and other associated processes in our animal model. After 6 weeks of TAA administration, TAA-treated livers from tumor-bearing mice showed the extensive appearance of portal–portal and central–portal fibrous septae, distortion of liver architecture and regenerative nodules (Figure 5A). However, a marked reduction in the amount of fibrous septae and of regenerative nodules was found in 4-MU-treated animals. In order to assess the extent of liver fibrosis, the Metavir score and Sirius Red staining were performed. We observed that untreated animals showed distortion of liver architecture, portal–portal and central–portal fibrous linkages, correlated with an F2-3 fibrosis degree, whereas 4-MU-treated mice showed a reduced amount of collagen with occasional portal–portal bridges (F1-2; Figure 5A).

In order to quantify the hepatic content of collagen, the ECM protein most abundantly accumulated in the fibrotic livers, tissue sections from TAA-treated animals were stained with Sirius Red and morphometric analysis was performed. A significant reduction in the Sirius Red^{+} area was found in 4-MU-treated mice when compared with non-treated mice (0.65 ± 0.08 vs 1.48 ± 0.11%; Figure 5B).

Liver fibrogenesis is characterized by trans-differentiation of HSCs. In addition, HSC-derived myofibroblasts, regarded as the main sources of ECM proteins as well as of pro-inflammatory cytokines in a fibrotic liver, are known to increase α-smooth muscle actin (α-SMA) expression levels according to the degree of their activation state. In order to address whether either the number of myofibroblasts in fibrous septae or/and the activation state of myofibroblasts might be affected by 4-MU treatment, the liver tissue obtained from 6-week TAA-treated mice was immunostained for α-SMA detection. A significant reduction in the α-SMA^{+} immunostained area was found in 4-MU when compared with non-treated mice (0.17 ± 0.02 vs 0.40 ± 0.04%; Figure 5C). These results suggest that the 4-MU therapy reduces the number and/or the activated state of myofibroblasts, cells playing a key role in liver fibrogenesis.

In vitro 4-MU treatment inhibits cell proliferation and induces apoptosis in fibroblast cell lines

In order to study the effect of 4-MU treatment in fibrosis development, we analyzed proliferation and apoptosis of hepatic fibroblasts and HSC as described in Materials and Methods section (Figure 6A). Proliferation was inhibited in all the studied doses of 4-MU in murine hepatic fibroblasts IZA2.1, rat CFSC-2G and human LX2 hepatic stellate cell lines. However, the apoptosis index was increased only with higher doses of 4-MU (5 mM) in the three cell lines.

Discussion

In this work, we show that 4-MU, a well-known HA synthesis inhibitor and a dietary supplement, is an effective antiproliferative and pro-apoptotic agent with antitumoral and antifibrotic effects both in vitro and in vivo. It is well known that endogenous HA synthesis is up-regulated during liver fibrosis, cirrhosis (Engstrom-Laurent et al. 1985; Frebourg et al. 1986) and cancer progression (Boregowda et al. 2006). Almost 90% of circulating HA is metabolized in the liver by HSC and sinusoidal cells; therefore, hepatic failure deteriorates HA clearance (Vrochides et al. 1996; Fraser et al. 1997). We hypothesize that hepatic HA accumulation plays a role in liver fibrogenesis and, consequently, in HCC development. The aim of our study was to determine whether 4-MU could be able to ameliorate liver fibrosis and HCC growth in an orthotopic mouse model.

First, we analyzed the expression of CD44, HA synthesis and binding capacity of Hepa129 tumor cells. We observed that Hepa129 cells bind to HA, in part through CD44, because HA binding was not completely abolished by anti-CD44 treatment, an HA-blocking antibody (KM81); therefore, it seems that other receptors may also be implicated, such as LYVE-1 and RHAMM (Day and Prestwich 2002). In addition, Hepa129 tumor cells produced higher amounts of HA as determined by the HA-BP and ELISA-like assays. These results are in agreement with other studies, where malignant tumors have high levels of HA (Toole 2002). Higher production of HA was associated with increased migration, metastases development and tumor survival (Toole 2002).

HCC generally arises in a cirrhotic liver (Pons-Renedo and Llovet 2003); it is, therefore, of great importance to investigate HCC development in association with a fibrotic microenvironment. For that reason, we established an orthotopic HCC animal model in mice with advanced fibrosis induced by TAA chronic intoxication. This model allows us to investigate the effect of inhibition of HA synthesis by 4-MU in a scenario that more closely mimic clinical liver cancer (Pons-Renedo and Llovet 2003). 4-MU therapy inhibits the growth of the main tumor mass by 35%, although statistically no significant differences were achieved between groups. However, 4-MU treatment significantly reduced the number of satellites nodules when compared with untreated tumor-bearing mice. In addition, histological analysis revealed that tumor tissue in animals treated with 4-MU presented extensive areas of necrosis, indicating tumor cell death, and tumor inflammatory infiltrate. Besides, we observed that 4-MU treatment was associated with a reduced development of severe ascites in mice with HCC and fibrosis.

In order to support these results, we carried out in vitro proliferation and apoptosis assays to evaluate the effect of 4-MU on murine (Hepa129 cells) and human (Hep3B and Huh7) HCC cell lines. As expected, and most likely because of the great amount of HA produced by Hepa129, 4-MU inhibited proliferation and induce the apoptosis of these cancer cells. The same tendency regarding the inhibition of cell proliferation and the induction of tumor cell apoptosis was observed in Hep3B cells, which also produced HA although in low amount. Contrarily, Huh7 cells that synthesize low amounts of HA presented a partial resistance to 4-MU treatment, confirming that 4-MU activity depends on the inhibition of HA synthesis (Kultti et al. 2009; Lokeshwar et al. 2010).

The toxicity of 4-MU was determined in vivo in healthy mice as well as in vitro in primary hepatocytes culture. The toxicity profile of 4-MU was investigated in mice for their general behavior and body weight with no signs of evident toxicity. No

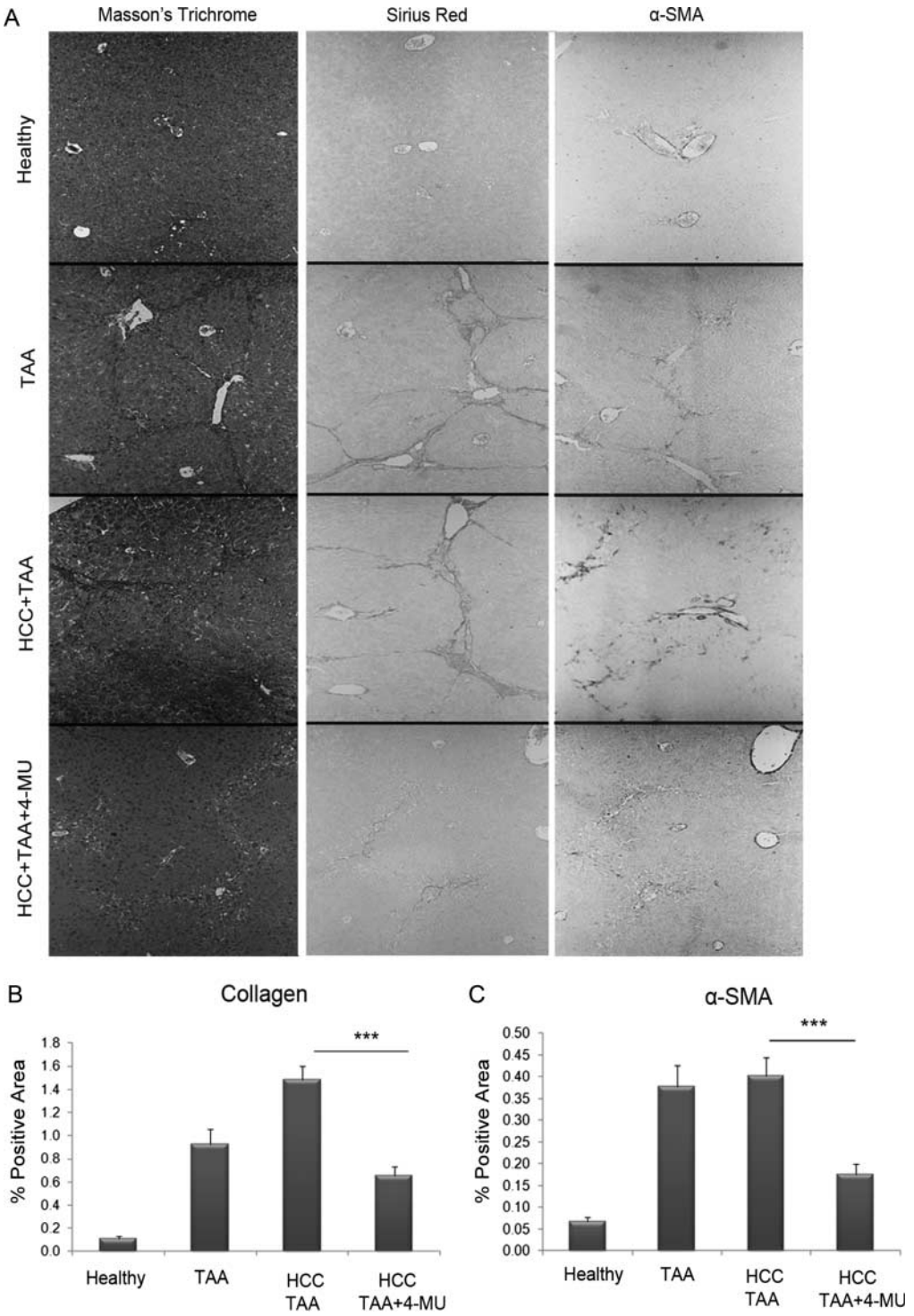

Fig. 5. Antifibrotic effects of 4-MU treatment. (**A**) Assessment of liver fibrosis: collagen type I lattices are visualized in blue by Masson's trichrome and in red by Sirius Red staining. α-SMA was detected by immunohistochemistry. Scale bar = 50 μm. (**B**) Quantification of collagen lattices by densitometry, ***$P < 0.001$. (**C**) Quantification of α-SMA-positive cells by densitometry, ***$P < 0.001$. Bars represent the average of measures of each group ± SEM. Experiments are shown as the average of three independent assays.

significant changes were observed in plasma ALT levels in all studied groups. In addition, hepatic architecture in healthy animals treated with 4-MU was well preserved and hepatocytes isolated from healthy mice were resistant to 4-MU toxicity in all doses analyzed. Therefore, we assume that 4-MU is well tolerated and has a very low profile of hepatic toxicity.

In agreement with others, we observed that in fibrotic livers HA is scattered and presented within fibrotic bridges

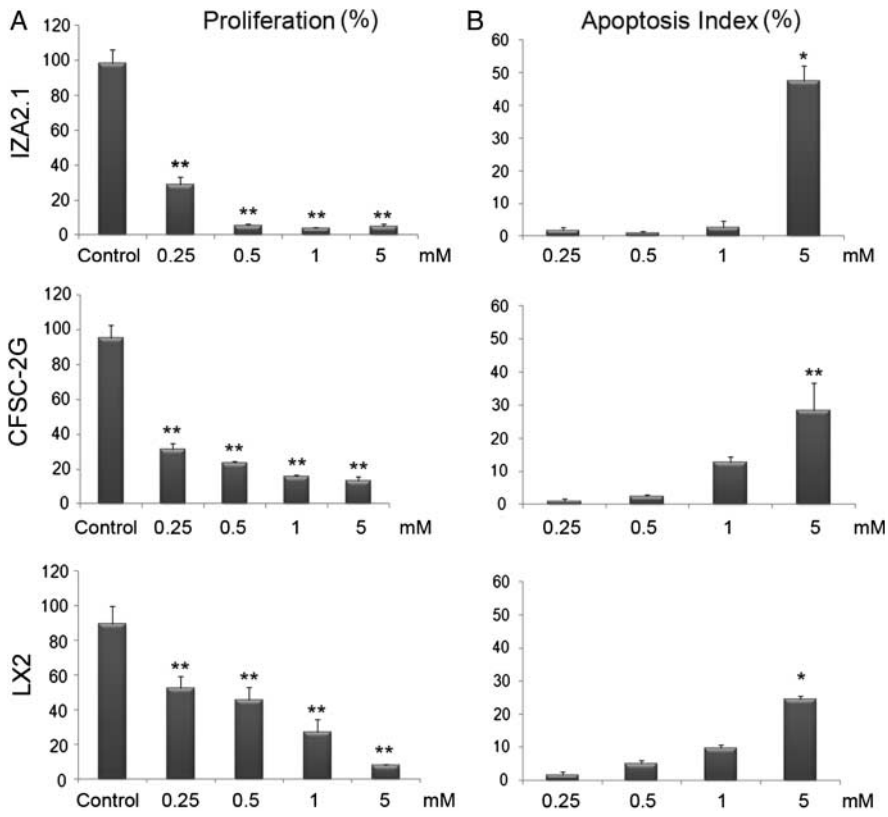

Fig. 6. (**A**) In vitro proliferation assay on IZA2.1 hepatic fibroblasts and rat (CFSC-2G) and human (LX2) HSCs, tested by 3H-thymidine incorporation at different 4-MU concentrations. Control: HBSS medium. $^{**}P < 0.01$. This experiment is representative of three independent experiments. Data are expressed as the mean ± SEM of proliferation average (measured in triplicate). (**B**) Apoptosis was tested in vitro by morphological features using acridin orange/ethidium bromide (right panel). Apoptosis index: % Apoptosis 4-MU − % Apoptosis control. $^{*}P < 0.05$, $^{**}P < 0.01$ vs control (not shown). Bars represent the average of measures of each group ± SEM. Experiments are shown as the average of three independent assays.

(Urashima et al. 1999; George et al. 2004). Both fibrosis and HCC increased the amount of HA present in the liver tissue and serum, which could be a result of increased synthesis and/or deficient clearance (Fraser et al. 1997). As expected, 4-MU treatment reduced the hepatic HA content and serum levels in mice with advanced fibrosis with HCC. These results might indicate that the effects induced by 4-MU treatment are closely related to its capability to inhibit HA synthesis. Hepa129 cells produced larger amounts of HA and 4-MU reduced not only intratumoral but also non-tumoral HA deposition. It has been observed that HA MW may determine its biological function (Toole 2004). We analyzed the MW of hepatic HA by fast protein liquid chromatography (FPLC) and observed that 4-MU seems not to affect HA function by altering its weight, but only its amount (not shown).

ECM synthesis and composition, in particular collagen fibrillar formation, are critical steps during hepatic fibrogenesis. In this sense, we showed in this work that 4-MU therapy ameliorates the degree of fibrosis in mice chronically intoxicated with TAA. Accordingly, tumor-bearing animals that received TAA showed the F2-3 fibrosis stage and those animals treated with 4-MU showed the F1-2 fibrosis stage as assessed by the Metavir score. Densitometric analyses of collagen deposition from tissues stained with Sirius Red were significantly reduced in 4-MU-treated mice when compared with untreated mice.

Myofibroblasts do normally accumulate in the parenchyma close to liver injury areas. Many of them most likely derive from resident HSCs, the main source of fibrillar collagen. By mean of immunohistochemical studies, a decrease in the number of α-SMA^{+} myofibroblasts was shown in fibrotic livers of 4-MU treated mice. In addition, when the action of 4-MU on hepatic myofibroblast-like or fibroblast cells was analyzed, we observed that all doses of 4-MU induced significant apoptosis and inhibited cell proliferation, indicating a high dependence on the synthesis of HA for survival, supporting the notion that 4-MU has an antifibrogenic activity. Recent studies have shown that HA is essential in differentiation of myofibroblast cells by regulating transforming growth factor (TGF)-β response, main mediator of fibrotic progression (Webber, Jenkins, et al. 2009; Webber, Meran, et al. 2009). Thus, further studies are needed to evaluate a possible mechanism involving 4-MU as a modulator of TGF-β response in the context of liver fibrosis.

In conclusion, our study shows that 4-MU, a well-known HA synthesis inhibitor, is a non-toxic compound that demonstrates strong anticancer effects and antifibrotic properties. Therefore, we suggest a role for 4-MU as an anticancer agent in HCC associated with advanced fibrosis.

Materials and methods

Animals, cells and reagents

Six-to-eight-week-old male C3H/He mice were purchased from Centro Atómico Ezeiza, Bs. As., Argentina. Animals were maintained at our Animal Resources Facilities (School of Biomedical Sciences, Austral University) in accordance with the experimental ethical committee and the NIH guidelines on the ethical use of animals. Hepa129 cells (HCC syngeneic with C3H/He mice) were kindly provided by Dr. Volker Schmitz (Bonn University, Germany) and grown in RPMI 1640 (GIBCO, Invitrogen Argentina, Buenos Aires, Argentina) with 10% fetal bovine serum (FBS). Hep3B (ATCC, Manassas, VA 20108, USA), Huh7 and LX2 (human HSCs were kindly provided by Dr. Scott Friedman, Mount Sinai, School of Medicine, NY) were grown in Dulbecco's modified Eagle's medium (DMEM; GIBCO) with 5% FBS. CFSC-2G cells (activated HSC lines) kindly provided by Dr. Marcos Rojkind (Albert Einstein College of Medicine) were grown in MEM (GIBCO) with 10% FBS. IZA2.1 (an immortalized hepatic fibroblast cell line) provided by Dr. Ignacio Melero (University of Navarra, Spain) was grown in DMEM (GIBCO) with 10% FBS. Primary culture of murine hepatocytes was obtained through liver perfusion with collagenase type V (Sigma-Aldrich, Buenos Aires, Argentina) and maintained in 70% DMEM–30% F12 medium with 10% FBS, 8.5 ng/mL choleric toxin, 10 ng/mL epidermal growth factor and 0.8 µg/mL hydrocortisone (De Smet et al. 1998). For in vitro toxicity study, these cells (5000/well) were incubated for 24 h and then treated with 4-MU (Sigma-Aldrich) at different concentrations (0.25, 0.5, 1 and 5 mM) or control vehicle solution [Hank's balanced salt solution (HBSS)] for additional 48 h.

CD44 expression and HA binding

Briefly, cells (5×10^5) were incubated with different mAbs: anti-mouse CD44 (an HA-binding blocker antibody, KM81, 1 µg/100 µL) and anti-mouse PE for Hepa129 cells and anti-human CD44-PE (dilution 1:11, DB105, Miltenyi-Lab Systems S. A. Buenos Aires, Argentina) for Hep3B and Huh7, respectively, or isotype control (BD Biosciences, Becton Dickinson Argentina, Buenos Aires, Argentina) on ice for 30 min. Cells were washed thoroughly with PBS–1% bovine serum albumin (BSA), fixed with 1% paraformaldehyde and subjected to flow cytometry (FACSCalibur, Becton Dickinson Immunocytometry Systems, San Jose, CA). HA binding was detected by incubation with HA-fluorescein isothiocyanate (FITC) (20 µg/100 µL, Calbiochem SA, Bs. As., Argentina), and CD44 displacement was performed by blockade with 10 µL/100 µL anti-CD44 (KM81) for 30 min. Hep3B and Huh7 as growth as adherent monolayer for all assay cells were harvested using a cell scraper in order to avoid cell-surface receptor cleavage. Analysis by flow cytometry was performed with a FACSAria flow cytometer (Becton Dickinson Immunocytometry Systems), and data were analyzed by WinMDI software (The Scripps Research Institute, La Jolla, CA).

Cell proliferation and apoptosis assays

For the proliferation assay, cells (2.5×10^5/well) were incubated in a 24-well plate with 4-MU at different concentrations (0.25, 0.5, 1 and 5 mM). After 48 h, cultures were pulsed with 5 µCi/mL [methyl-3H] thymidine for the last 6 h. Then, cells were lysed and the incorporation of radioactivity was measured in a liquid scintillation β-counter (Beckman LS 6500). Morphological features associated with apoptosis were analyzed by acridine orange and ethidium bromide staining. Cells (Hepa129, Hep3B, Huh7, IZA2.1, CFSC-2G, LX2 and freshly isolated hepatocytes) were treated with 4-MU as in the proliferation assay. Forty-eight hours later, cells were resuspended in the dye mixture (100 µg/mL acridine orange and 100 µg/mL ethidium bromide in PBS) and visualized by fluorescence microscopy (Nikon Eclipse E800, Nikon, Buenos Aires, Argentina). The percentage of apoptotic cells or apoptotic index was calculated as: apoptotic cells (%) = (total number of cells with apoptotic nuclei/total number of cells counted) × 100. The percentage of apoptosis for each treatment was calculated by subtraction of spontaneous apoptosis from induced apoptosis [treated apoptotic cells (%) − untreated cells (%)] (Alaniz et al. 2006). In order to confirm apoptosis results by acridine orange and ethidium bromide staining, Annexin V kit detection (BD Pharmingen, Becton Dickinson, Argentina) was used (Alaniz et al. 2006). Analysis by flow cytometry was performed with a FACSAria flow cytometer (Becton Dickinson Immunocytometry Systems), and data were analyzed by WinMDI software (The Scripps Research Institute).

HA quantification by an ELISA-like assay

HA from cell-free supernatants, serum and liver tissues were measured using a competitive ELISA-like assay as described elsewhere (Cordo-Russo et al. 2009). Briefly, 96-well microplates (Nunc, Lobov y Cia S.A, Ciudad de Buenos Aires, Argentina) were coated with 100 µg/mL of HA (CPN spol.s.r. o., Czech Republic). Then, wells were incubated with 25 µL of sample (serum diluted 1/50, tissues diluted 1/800) or standard HA (0–1 µg/mL), in the presence of 0.75 µg/mL of biotinylated HA-BP (bHA-BP; # 385911, Calbiochem) at 37°C for 4 h and then washed with PBS–0.05% Tween-20. The bHA-BP bound to the wells was determined using an avidin–biotin detection system (Sigma-Aldrich, Buenos Aires, Argentina). Sample concentrations were calculated from a standard curve generated by plotting the absorbance at 490 nm against the concentration of HA (Cordo-Russo et al. 2009). Cell-free culture supernatants were obtained from tumor cell treated or not treated with 4-MU at different concentrations (0.25, 0.5, 1 and 5 mM) at 12 h for Hepa129 (10^6 cells/mL) or 24 h for Hep3B and Huh7 (10^6 cells/mL); the HA level was normalized to the supernatant volume. For liver HA analysis (100 mg of tissue), the GAG extract was obtained as described (Cordo-Russo et al. 2009). Briefly, frozen samples of a liver (50 mg each) were suspended in 0.1 M ammonium acetate, pH 7.0, and digested with 20 U/mL of protease K (EC 3.4.21.64 Finnzymes Espoo, Finland), at 60° C for 2 h followed by enzyme inactivation by heating at 95°C for 5 min. GAGs were precipitated with ethanol 96% at −20° C overnight. After centrifugation at 10,000 × *g* at 4°C for 45 min, pellets were washed with ethanol and resuspended in PBS. HA from serum was obtained from blood with drawn

by retro-orbital bleeding, centrifuged at 0.8 × *g* for 20 min at 4°C, and the decanted serum was stored at −80°C.

Experimental model

Fibrosis was induced by intraperitoneal (i.p.) injections of TAA (at a dose of 200 mg/kg; Sigma-Aldrich) thrice weekly for 42 days (Figure 3A; Salguero Palacios et al. 2008). On day 30, fibrotic mice were anesthetized and orthotopic tumors were established by subcapsular inoculation of 1.25×10^5 Hepa129 cells into the left liver lobe by laparotomy (Kornek et al. 2008). Two days before tumor implantation, a group of mice received 4-MU treatment by i.p. injection at a dose of 20 mg/kg per day, for 14 days (HCC + TAA + 4-MU group). A group of mice with fibrosis induced by TAA was also included as control (TAA group). Twelve days after tumor implantation, mice were sacrificed, and ascites grade (mild, moderated, severe and hemorrhagic) and tumor volume and numbers of HCC satellites were quantified.

Pathology

Formol-fixed liver samples were embedded in paraffin and 5 µm sections were stained by hematoxylin/eosin (H&E), Masson's trichrome and Sirius Red. Fibrosis was assessed according to the Metavir scoring system (no fibrosis F0, cirrhosis F4; Beaussier et al. 2005). The analysis was performed in a blinded fashion by a single pathologist.

HA staining

HA staining was performed as described elsewhere (Jameson et al. 2005). Briefly, paraffin liver sections were incubated with 3% H_2O_2–methanol for 30 min at room temperature (RT) to block endogenous peroxidase, followed by avidin, biotin and protein-blocking solution (Vector, BIOARS S.A. Ciudad de Buenos Aires, Argentina). Then, 5 µg/mL of bHA-BP (# 385911, Calbiochem) diluted in 1% BSA–PBS was applied for 1 h. Negative controls were stained with bHA-BP and pretreated with 100 U/mL of Streptomyces hyaluronidase (# 385931, Calbiochem) at 37°C for 30 min. Peroxidase complex (Sigma) 1:10 in PBS was used as a revealing system. The signal was detected by 0.1% diaminobenzidine (Sigma-Aldrich, Buenos Aires, Argentina), 4% glucose, 0.08% $ClNH_4$, 5% nickel ammonium sulfate in 0.2 M AcNa and 0.05% H_2O_2.

Immunohistochemistry for α-SMA

Briefly, paraffin liver sections were incubated with 3% H_2O_2–methanol for 30 min at RT to block endogenous peroxidase, followed by avidin, biotin and protein-blocking solution (Vector). Sections were incubated with a rabbit polyclonal antibody to α-SMA (Abcam, Tecnolab S.A. Buenos Aires, Argentina) 1/10 in 0.2% BSA–0.1% Triton X-100 in PBS over night (O.N.) at 4°C, and a biotinylated anti-rabbit secondary antibody (Vector) 1/100 in 0.2% BSA in PBS at RT for 1 h. The signal was detected as described for HA staining (Materials and Methods section).

Collagen and α-SMA quantification

α-SMA-positive fibroblasts and collagen fibrils from liver sections were detected by analyzing 50 images/section ($n = 4$) taken at 200× (Nikon) and percentage of the positive area was calculated with ImageJ software (National Institutes of Health, Bethesda, MD).

Transaminases measurement

Serum alanine transaminase (ALT) was measured using an ARCHITECT® (Abbott, Buenos Aires, Argentina) autoanalyzer.

Cytotoxicity assay

Freshly isolated hepatocytes or Hepa129 cells were plated on 5000 hepatocytes/well, and Cytotoxicity Detection Kit PLUS (LDH, Roche, Buenos Aires, Argentina) was used to detect lactate dehydrogenase (LDH) activity. Absorbance was read at 490 nm. Toxicity (%) = (experimental value − low control)/(high control − low control) × 100, where low control means cells with assay medium and high control cells with assay medium and lysis buffer.

Statistic analysis

Values were expressed as the mean ± SEM. The Mann–Whitney or Kruskall–Wallis (ANOVA) tests were used to evaluate the statistical differences between two groups or more than two groups, respectively. A *P*-value of <0.05 was considered as significant. Prism software (Graph Pad, San Diego, CA) was employed for the statistical analysis.

Funding

This work was supported by grants from Mizutani Foundation for Glycoscience (80072), Austral University, Agencia Nacional de Promoción Científica y Tecnológica (PICT-2006-1882; PICT-2005-34788, PICT 2007-00736, PICTO-CRUP 2005-31179 and PICT 2010-2818).

Acknowledgements

We would like to thank Soledad Arregui and Guillermo Gastón for their expert technical assistance.

Conflict of interest

None declared.

Abbreviations

ALT, alanine transaminase; bHA-BP, biotinylated HA-BP; BSA, bovine serum albumin; DMEM, Dulbecco's modified Eagle's medium; ECM, extracellular matrix; ELISA, enzyme-linked immunosorbent assay; FBS, fetal bovine serum; FITC, fluorescein isothiocyanate; FPLC, fast protein liquid chromatography; GAG, glycosaminoglycan; HA, hyaluronan; HA-BP, HA binding protein; HBSS, Hank's balanced salt solution; HCC, hepatocellular carcinoma; H&E, hematoxylin/eosin; HMW, high MW; HSC, hepatic stellate cells; i.p., intraperitoneal; LDH, lactate dehydrogenase; mAb, monoclonal

antibody; 4-MU, 4-methylumbelliferone; MW, molecular weight; O.N., over night; RT, room temperature; SMA, smooth muscle actin; TAA, thioacetamide; TGF, transforming growth factor.

References

Alaniz L, Garcia MG, Gallo-Rodriguez C, Agusti R, Sterin-Speziale N, Hajos SE, Alvarez E. 2006. Hyaluronan oligosaccharides induce cell death through PI3-K/Akt pathway independently of NF-κB transcription factor. *Glycobiology.* 16:359–367.

Alaniz L, Garcia M, Rizzo M, Piccioni F, Mazzolini G. 2009. Altered hyaluronan biosynthesis and cancer progression: An immunological perspective. *Mini Rev Med Chem*. 9:1538–1546.

Bataller R, Brenner DA. 2005. Liver fibrosis. *J Clin Invest*. 115:209–218.

Beaussier M, Wendum D, Fouassier L, Rey C, Barbu V, Lasnier E, Lienhart A, Scoazec JY, Rosmorduc O, Housset C. 2005. Adaptative bile duct proliferative response in experimental bile duct ischemia. *J Hepatol*. 42:257–265.

Boregowda RK, Appaiah HN, Siddaiah M, Kumarswamy SB, Sunila S, Thimmaiah KN, Mortha K, Toole B, Banerjee S. 2006. Expression of hyaluronan in human tumor progression. *J Carcinog*. 5:2.

Cordo-Russo R, Garcia MG, Barrientos G, Orsal AS, Viola M, Moschansky P, Ringel F, Passi A, Alaniz L, Hajos S, et al. 2009. Murine abortion is associated with enhanced hyaluronan expression and abnormal localization at the fetomaternal interface. *Placenta*. 30:88–95.

Day AJ, Prestwich GD. 2002. Hyaluronan-binding proteins: Tying up the giant. *J Biol Chem*. 277:4585–4588.

De Smet K, Beken S, Vanhaecke T, Pauwels M, Vercruysse A, Rogiers V. 1998. Isolation of rat hepatocytes. *Methods Mol Biol*. 107:295–301.

El-Serag HB, Rudolph KL. 2007. Hepatocellular carcinoma: Epidemiology and molecular carcinogenesis. *Gastroenterology.* 132:2557–2576.

Engstrom-Laurent A, Loof L, Nyberg A, Schroder T. 1985. Increased serum levels of hyaluronate in liver disease. *Hepatology.* 5:638–642.

Fraser JR, Laurent TC, Laurent UB. 1997. Hyaluronan: Its nature, distribution, functions and turnover. *J Intern Med*. 242:27–33.

Fraser JR, Laurent TC, Pertoft H, Baxter E. 1981. Plasma clearance, tissue distribution and metabolism of hyaluronic acid injected intravenously in the rabbit. *Biochem J*. 200:415–424.

Frebourg T, Delpech B, Bercoff E, Senant J, Bertrand P, Deugnier Y, Bourreille J. 1986. Serum hyaluronate in liver diseases: Study by enzymoimmunological assay. *Hepatology.* 6:392–395.

Friedman SL. 2008. Mechanisms of hepatic fibrogenesis. *Gastroenterology.* 134:1655–1669.

George J, Tsutsumi M, Takase S. 2004. Expression of hyaluronic acid in N-nitrosodimethylamine induced hepatic fibrosis in rats. *Int J Biochem Cell Biol.* 36:307–319.

Guo N, Li X, Mann MM, Funderburgh ML, Du Y, Funderburgh JL. 2010. Hyaluronan synthesis mediates the fibrotic response of keratocytes to transforming growth factor beta. *J Biol Chem*. 285:32012–32019.

Jameson JM, Cauvi G, Sharp LL, Witherden DA, Havran WL. 2005. Gammadelta T cell-induced hyaluronan production by epithelial cells regulates inflammation. *J Exp Med*. 201:1269–1279.

Kakizaki I, Kojima K, Takagaki K, Endo M, Kannagi R, Ito M, Maruo Y, Sato H, Yasuda T, Mita S, et al. 2004. A novel mechanism for the inhibition of hyaluronan biosynthesis by 4-methylumbelliferone. *J Biol Chem*. 279:33281–33289.

Kornek M, Raskopf E, Tolba R, Becker U, Klöckner M, Sauerbruch T, Schmitz V. 2008. Accelerated orthotopic hepatocellular carcinomas growth is linked to increased expression of pro-angiogenic and prometastatic factors in murine liver fibrosis. *Liver Int*. 28:509–518.

Kultti A, Pasonen-Seppänen S, Jauhiainen M, Rilla KJ, Kärnä R, Pyöriä E, Tammi RH, Tammi MI. 2009. 4-Methylumbelliferone inhibits hyaluronan synthesis by depletion of cellular UDP-glucuronic acid and downregulation of hyaluronan synthase 2 and 3. *Exp Cell Res*. 315:1914–1923.

Lokeshwar VB, Lopez LE, Munoz D, Chi A, Shirodkar SP, Lokeshwar SD, Escudero DO, Dhir N, Altman N. 2010. Antitumor activity of hyaluronic acid synthesis inhibitor 4-methylumbelliferone in prostate cancer cells. *Cancer Res*. 70:2613–2623.

McKee CM, Penno MB, Cowman M, Burdick MD, Strieter RM, Bao C, Noble PW. 1996. Hyaluronan (HA) fragments induce chemokine gene expression in alveolar macrophages. The role of HA size and CD44. *J Clin Invest*. 98:2403–2413.

Morohashi H, Kon A, Nakai M, Yamaguchi M, Kakizaki I, Yoshihara S, Sasaki M, Takagaki K. 2006. Study of hyaluronan synthase inhibitor, 4-methylumbelliferone derivatives on human pancreatic cancer cell (KP1-NL). *Biochem Biophys Res Commun*. 345:1454–1459.

Noble PW. 2002. Hyaluronan and its catabolic products in tissue injury and repair. *Matrix Biol*. 21:25–29.

Pons-Renedo F, Llovet JM. 2003. Hepatocellular carcinoma: A clinical update. *MedGenMed*. 5:11.

Rampone B, Schiavone B, Confuorto G. 2010. Current management of hepatocellular cancer. *Curr Oncol Rep*. 12:186–192.

Safadi R, Friedman SL. 2002. Hepatic fibrosis–role of hepatic stellate cell activation. *MedGenMed*. 4:27.

Salguero Palacios R, Roderfeld M, Hemmann S, Rath T, Atanasova S, Tschuschner A, Gressner OA, Weiskirchen R, Graf J, Roeb E. 2008. Activation of hepatic stellate cells is associated with cytokine expression in thioacetamide-induced hepatic fibrosis in mice. *Lab Invest*. 88: 1192–1203.

Stern R. 2005. Hyaluronan metabolism: A major paradox in cancer biology. *Pathol Biol (Paris)*. 53:372–382.

Takeda S, Aburada M. 1981. The choleretic mechanism of coumarin compounds and phenolic compounds. *J Pharmacobiodyn*. 4:724–734.

Tammi MI, Day AJ, Turley EA. 2002. Hyaluronan and homeostasis: A balancing act. *J Biol Chem*. 277:4581–4584.

Toole BP. 2002. Hyaluronan promotes the malignant phenotype. *Glycobiology.* 12:37R–42R.

Toole BP. 2004. Hyaluronan: From extracellular glue to pericellular cue. *Nat Rev Cancer.* 4:528–539.

Turley EA, Noble PW, Bourguignon LY. 2002. Signaling properties of hyaluronan receptors. *J Biol Chem*. 277:4589–4592.

Twarock S, Freudenberger T, Poscher E, Dai G, Jannasch K, Dullin C, Alves F, Prenzel K, Knoefel WT, Stoecklein NH, et al. 2011. Inhibition of oesophageal squamous cell carcinoma progression by in vivo targeting of hyaluronan synthesis. *Mol Cancer.* 10:30.

Urakawa H, Nishida Y, Wasa J, Arai E, Zhuo L, Kimata K, Kozawa E, Futamura N, Ishiguro N. 2011. Inhibition of hyaluronan synthesis in breast cancer cells by 4-methylumbelliferone suppresses tumorigenicity in vitro and metastatic lesions of bone in vivo. *Int J Cancer.* doi: 10.1002/ijc.26014.

Urashima S, Tsutsumi M, Shimanaka K, Ueshima Y, Tsuchishima M, Itoh T, Kawahara H, Takase S. 1999. Histochemical study of hyaluronate in alcoholic liver disease. *Alcohol Clin Exp Res*. 23:56S–60S.

Vrochides D, Papanikolaou V, Pertoft H, Antoniades AA, Heldin P. 1996. Biosynthesis and degradation of hyaluronan by nonparenchymal liver cells during liver regeneration. *Hepatology.* 23:1650–1655.

Webber J, Jenkins RH, Meran S, Phillips A, Steadman R. 2009a. Modulation of TGFbeta1-dependent myofibroblast differentiation by hyaluronan. *Am J Pathol*. 175:148–160.

Webber J, Meran S, Steadman R, Phillips A. 2009b. Hyaluronan orchestrates transforming growth factor-β1-dependent maintenance of myofibroblast phenotype. *J Biol Chem*. 284:9083–9092.

West DC, Shaw DM, Lorenz P, Adzick NS, Longaker MT. 1997. Fibrotic healing of adult and late gestation fetal wounds correlates with increased hyaluronidase activity and removal of hyaluronan. *Int J Biochem Cell Biol*. 29:201–210.

Yoshihara S, Kon A, Kudo D, Nakazawa H, Kakizaki I, Sasaki M, Endo M, Takagaki K. 2005. A hyaluronan synthase suppressor, 4-methylumbelliferone, inhibits liver metastasis of melanoma cells. *FEBS Lett*. 579: 2722–2726.